The Potential for Soil Carbon Sequestration in the San Joaquin Delta

Zahira H. Chaudhry

ABSTRACT

Soil texture analysis can be used as a predictor of soil carbon content in managed agricultural peat soils in the San Joaquin Delta. I conducted a soil texture analysis of 65 soil samples from four different land uses: pastureland, wetland, corn, and alfalfa. Soil samples were collected at various sites across the Delta using soil core augering, taken at 5 m intervals along three 20 m transects at each site. Soil samples were processed then analyzed using the hydrometer method to determine the percent composition of clay, sand and silt of each soil sample. I ran a one-way ANOVA to determine the distribution of clay, sand and silt content across the three depth categories and to compare distributions between drained and flooded soils. Linear regression analysis illustrated the relationship between the percentage of clay, sand and silt content and the percentage of calculated carbon content. Soils with higher clay content were expected to hold a higher amount of carbon, but no trends between soil carbon and clay were found. Negative trends between silt and carbon may indicate the importance of silt as a source of redox active minerals that may limit soil carbon sequestration. Positive correlations between sand and carbon may illustrate that sandy soils have the highest potential for soil carbon sequestration. Overall, management practices such as reflooding are the best options to aid soil carbon sequestration in the San Joaquin Delta.

KEYWORDS

peatland, soil texture, clay, flooding, redox active minerals

INTRODUCTION

As climate change accelerates, the amount of carbon dioxide (CO_2) and other greenhouse gases in the atmosphere increase the risk of global climate disaster. To reverse or slow climate change, engineering technologies to reduce greenhouse gas emissions, including wetland ecosystem restoration, can be utilized to capture atmospheric carbon (C) and sequester the gas in soil (Knox et al. 2014). These soil C sequestration technologies provide a multitude of benefits, including reducing the amount of CO_2 in the atmosphere. Organic-rich soil is the most common soil type currently used in this soil C sequestration research, as restoring organic-rich soils both sequesters new C and protects residual C (Deverel et al. 2014, Hemes et al. 2019). However, numerous gaps in this research inhibit full implementation due to the unknown limitations to sequestration in these heterogeneous soil systems, as well as the effects of C sequestration strategies on other biogeochemical pathways or biophysical feedbacks to climate change (Hemes et al. 2019). Soil C sequestration can radically change the landscape of an ecosystem and political, cultural and economic constraints must be considered along with other environmental impacts, including non-CO_2 greenhouse gas emissions (Smith 2004).

A particularly important soil type for C sequestration are peatlands soils, as they are rich in organic matter and although they account for only ~3% of the world's terrestrial soil, they hold 21% of the world's soil C (Leifeld and Menichetti 2018). These high levels of organic matter make peat soils fertile agricultural zones and, as a result, they aree often drained for agricultural use (Pronger et. al. 2014). Drained peatland soils are ideal to measure soil C dynamics because they are not only large sources of greenhouse gases, but also large potential sinks for them too (Hemes et al. 2019). To understand the relationship between the potential for soil C sequestration across a range of degraded peatland soils, there must be more research on the effects of soil characteristics on soil C accumulation and loss in these systems. In particular, the relationship between soil texture and soil C in peatland soils will help us understand the potential for soil C sequestration in peatlands.

Soil texture is differentiated by particle size, and soil texture analysis is used to determine the ratios of clay, sand, and silt in a particular soil. Clay particles have the highest surface area while sand particles have the lowest surface area. The higher surface area of clay increases particle

reactivity and stabilizes soil organic C. High surface area also allows clay particles to form aggregates that protect the soil C from decomposition (Schimel et al. 1994). Soil C and soil texture have a linear relationship, thus soil C increases with increasing clay content (Schimel et al. 1994). Peatlands deposited in a river delta typically contain high amounts of alluvium silt and clay deposits (Deverel et al. 2015). Thus, peatlands with higher clay content are expected to hold a higher percentage of soil C.

Management practices of agricultural peatlands utilize drainage of flooded wetlands to increase agricultural productivity. However, peatland draining can also damage soil health and release greenhouse gases into the atmosphere (Landry and Rochefort 2012). After drainage, the peat is aerated and has a higher oxygenation rate than the flooded peat. This higher oxygenation rate reduces the volume of the soil and increases soil compaction, which can cause ground subsidence of 3.5 to 10 cm per year (Landry and Rochefort 2012). Peatland decomposition also increases with drainage as the majority of the peat profile is now aerated, modifying the surface-level microbial communities to decompose peat and oxidize soil C faster. Drainage also changes the surface vegetation on the peatland, which further alters microbial communities and accelerates decomposition (Landry and Rochefort 2012). Lastly, several studies have measured an increased amount of CO_2 released into the atmosphere after peatland drainage (Moore and Dalva 1993, Silvola et al. 1996). To summarize, drained peatlands quickly transition from C sinks to C sources due to a reduction in anaerobic processes and increased decomposition (Ramchunder et al. 2009).

In this study, I will investigate if clay content is a predictor of soil C accumulation in managed peatland ecosystems. I will also further study if this potential for C sequestration in impacted by land management or other soil texture parameters. Since the field of C sequestration is still largely hypothetical, this project provides key insights into the potential and the limits of C sequestration in peatland soils.

METHODS

Study Site

The study site is the Sacramento-San Joaquin Delta region of Northern California (hereafter referred to as the Delta). The Delta has a temperate Mediterranean climate with hot and dry summers and cold, wet winters with a heavy rainy season**.** The Delta's historical mean annual temperature is 15.1° C and has a yearly average rainfall of 326 mm (McNicol et al. 2016). The Delta's close proximity to the convergence of the Sacramento and San Joaquin Rivers creates an ideal site for alluvial deposits. Some areas of the Delta experience seasonal flooding, while others remain permanently inundated.The Delta's fertility makes it particularly attractive to farmers and pasture utilization operations.

Large-scale agricultural development began in the region during the late 1800's, spurring the building of a levee system that prevented frequent flooding of the land. Today, the 57 islands and land tracts that comprise the Delta are protected from flooding by a system of levees that stretch to be 1,100 miles long. After lands were drained for agricultural use, continuously high rates of peat oxidation and compaction lead to substantial soil subsidence, increasing the stress on this complex levee system (Drexler et al. 2009). This stress, together with sea-level rise, greatly increases the vulnerability of these levees to collapse, which could be detrimental to the yearly $5.2 billion economic output of the Sacramento-San Joaquin Delta region (Delta Protection Commission 2012). In addition to lands used for agriculture, wetland restoration projects have been implemented to reverse soil subsidence and reduce risk of levee failure (Hemes et al. 2019, Knox et al. 2015). This diversity of land uses, soil C values, and soils types across a small geographical region (~35 km across; ~60 km^2 area) provide an excellent sample site to explore the C sequestration potential of peatland soils.

Site Selection

Soil samples were collected by T. Anthony in 2016 at nine different sites around the Delta Region. The nine sites were selected to represent the various land uses present across the

Delta. The nine sites are Bouldin 1, Bouldin 2, Bouldin Corn, Sherman, Sherman Pasture, Twitchell, East End, West Pond, and Mayberry (Figure A1). The soil samples were collected at either the drained agricultural sites or the flooded and restored wetland sites. Drained agricultural sites account for approximately 52% of the Delta's land use (Delta Protection Commission 2012). These sites include were found on Bouldin, Sherman, and Twitchell Islands and had three different land uses: continuous corn, continuously grazed pasture and perennial alfalfa. The continuous corn site was Bouldin Corn. The perennial alfalfa sites were Bouldin 1, Bouldin 2 and Twitchell. The continuously grazed pasture sites included Sherman and Sherman Pasture.

The wetland sites are located on Twitchell and Sherman Islands, but each wetland was restored at different times and had previous land use histories. West Pond wetland was restored in 1997 and the layer accumulated since restoration was largely undecomposed plant debris with a Histosol beneath. Prior to restoration, West Pond was used for agriculture land beginning in the mid-19th century and its primary purpose was to grow corn (Miller et al. 2008, Fleck et al. 2004). Mayberry is also a wetland site that was previously a pasture before its wetland restoration in 2010. East End wetland was previously used as a continuous corn field and was restored to a wetland in 2014 (Chamberlain et al. 2018, Eichelmann et al. 2018).

Soil Sampling and Analysis

Individual soil samples (n = 262) were collected using a soil auger. We collected soil samples along three 20 m transects per site, with five locations per transect separated by 5 m intervals. Visible organic surface litter was removed prior to soil sampling. At each coring location, cores were collected at 0-15 cm and 15-30 cm depths for flooded soils totaling 30 samples per site. Soils were processed within 24 hours of collection with the exception of air-dried analyses.

In preparation for C and nitrogen analyses, soil samples were air-dried, sieved to < 2 mm, and underwent root-picking to remove visible organic matter before being ground into a fine powder. Flooded peat soil samples were removed of large undecomposed organic material before sieving. Drained peat soils had highly decomposed organic material and no high amounts of plant material. Samples were then analyzed in duplicate for total C and nitrogen on a CE

Elantech elemental analyzer (Lakewood, New Jersey). 262 soil samples were collected and sixty five had enough volumetric content (>50g) for soil core analysis. The soil cores were part of a larger experiment looking at agricultural soil C sequestration rates in the San Joaquin Delta Region.

Data Collection

Soil Texture Analysis

To analyze the soil samples for texture analysis, I followed a protocol for soil texture analysis using the hydrometer method (Appendix B). First, I created a solution for each soil sample. The solution consisted of approximately 50 grams of the soil sample, 100 ml of 1*N* sodium hexametaphosphate and 200 ml of deionized water. The solution was placed on the shaker for 24 hours to ensure the creation of an even solution. After adequate shaking, the soil solution was transferred into a 1000 ml graduated cylinder and filled to the 1000 ml mark with deionized water. I then mixed the solution with a metal plunger. After removing the plunger from the solution, I began timing and placed the glass hydrometer in the solution to take readings at various time intervals. The first reading was taken at 30 seconds, the second was taken at 60 seconds, the third reading was taken at 90 minutes and the final reading was taken at 24 hours. For each set of soil texture analysis samples, a blank graduated cylinder containing 100 ml of 1*N* sodium hexametaphosphate and 900 ml of deionized water was also plunged and hydrometer readings were taken at the appropriate time intervals. Blank samples also had temperature readings taken at the same time intervals as the hydrometer readings. After all hydrometer and temperature values were recorded, the soil solutions were disposed of in a soil settling bucket and the graduated cylinders were cleaned.

Data Analysis

Analysis of soil texture data was performed using JMP Pro 13 (SAS Institute) and corresponding calculations developed by Gee and Bauder 1986. To account for differences in solution density with temperature and to interpret the data collected via the hydrometer method, I

needed to convert the corresponding hydrometer values in an excel spreadsheet. First, I calculated the average of the three 30 second hydrometer readings for each sample, resulting in one 30 second average value per soil sample (g/L). Next, I calculated the concentration of soil particles in solution at 30 seconds (C(30), in g/L) by subtracting the average of the 30 second readings of the appropriate blank sample from the average of the 33 second hydrometer readings for each sample. Next, I calculated the effective hydrometer depth (h') value by multiplying the average of the three 30 second hydrometer readings for each sample by the constant -0.164 and adding a constant 16.3, representative of a standard ASTM 152H hydrometer. I then calculated the sedimentation parameter (θ) value by multiplying h' by a constant *B* (a function of fluid viscosity (g cm^{-1} s^{-1}), the gravitational constant (cm/s^2), soil particle density (cm/s^2), and solution density (cm/s^2) and raising the value to the half power and multiplying the product by 1000. To get the percent of soil in solution at mean particle size in suspension at 30 seconds (X30), I multiplied θ by 1.414. I calculated the percent sand (Px) value by dividing the mass by the C(30) value. I repeated these calculations at different time intervals to get silt and clay values at various time intervals (90 minutes for silt, 24 hour for clay). The final values were used to calculate the percent composition of clay, sand, and silt of each sample.

To analyze the data from the above calculations, I used JMP Pro 13 software to run a one-way ANOVA and produce figures to test differences across depths and flooded status for clay, sand, and silt content. I also used a one-way ANOVA to test soil C differences across the three different depth categories and in the flooded and drained categories. Next, I used JMP to conduct linear regressions to illustrate the correlation between soil texture and soil C. The correlations were used to explore the relationship between the various percentages of clay, sand and silt and the percentage of C, as well as the effects of flooding and drainage on these values.

RESULTS

Soil Texture Values

Clay

Clay values differed significantly across the various depth categories ($p<0.01$). The mean and standard error of clay values at each were 23% +/- 1.5 % at 0-15 cm, 24% +/- 2.1 % at 15-30 cm and 15% +/- 2.5 % at 30-60 cm (Figure 1a). Clay values differed significantly between flooded (mean: 30% +/- 1.3%) and drained (mean: 20% +/- 2.8%) sites (Figure 1b).

(a) **(b)**

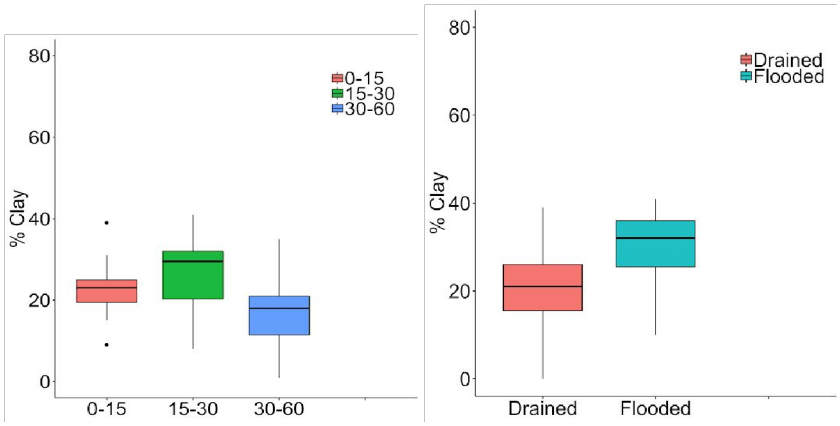

Figure 1. Difference in clay content across soil depth and flooding status. Box-and-whisker plot comparisons of percent clay content values across: (a) depth categories of 0-15, 15-30, and 30-60 cm and (b) drained and flooded soils. The box indicates the middle 50% (between 1st and 3rd quartile) of data values, the top whisker indicates the upper 25% of data valued, and the bottom whisker indicates the lowest 25% of data values. Outliers (values great than 1.5 times the interquartile range above the median or less than 1.5 times the interquartile range below the median) are included in the whiskers.

Silt

Silt values did not differ significantly across the various depth categories ($p<0.001$). The mean and standard error values for each depth of silt samples were 49% +/- 1.9% at 0-15 cm, 47% +/- 1.4% at 15-30 cm, and 51% +/- 2.9% at 30-60 cm (Figure 2a). Silt values had a higher range (30 to 69%)

at 30-60cm depths when compared to surface values. Drained (mean: 50% +/- 1.1%) soils had significantly higher silt values than flooded (mean: 40% +/- 1.5%) sites (Figure 2b).

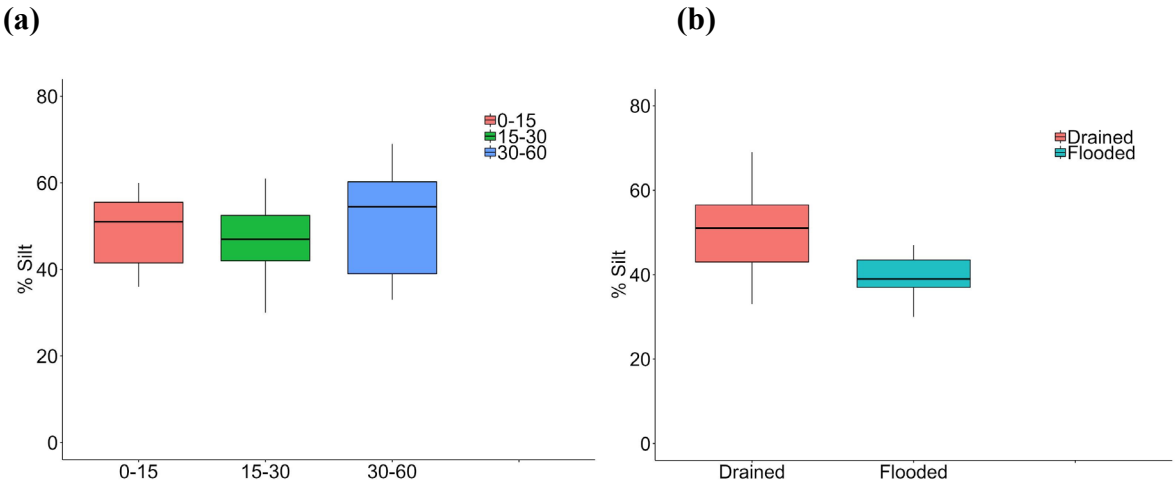

Figure 2. Difference in silt content across soil depth and flooding status. Box-and-whisker plot comparisons of percent silt content values across: (a) depth categories of 0-15, 15-30, and 30-60 cm and (b) drained and flooded soils. The box indicates the middle 50% (between 1st and 3 rd quartile) of data values, the top whisker indicates the upper 25% of data valued, and the bottom whisker indicates the lowest 25% of data values. Outliers (values great than 1.5 times the interquartile range above the median or less than 1.5 times the interquartile range below the median) are included in the whiskers.

Sand

Sand values did not differ significantly across the various depth categories as the p value was insignificant. The mean value for each depth of sand samples were 28% +/- 2.1% at 0-15 cm, 29% +/- 2.2% at 15-30 cm and 35% +/- 4.2% at 30-60cm (Figure 3a). Sand values had a higher range (36 to 60%) at 30-60 cm depths when compared to surface values. Sand had the highest variability of all soil textures within the depths. There were no differences across drained (30% +/- 1.8%) and flooded sites (30% +/- 2.7%) (Figure 3b).

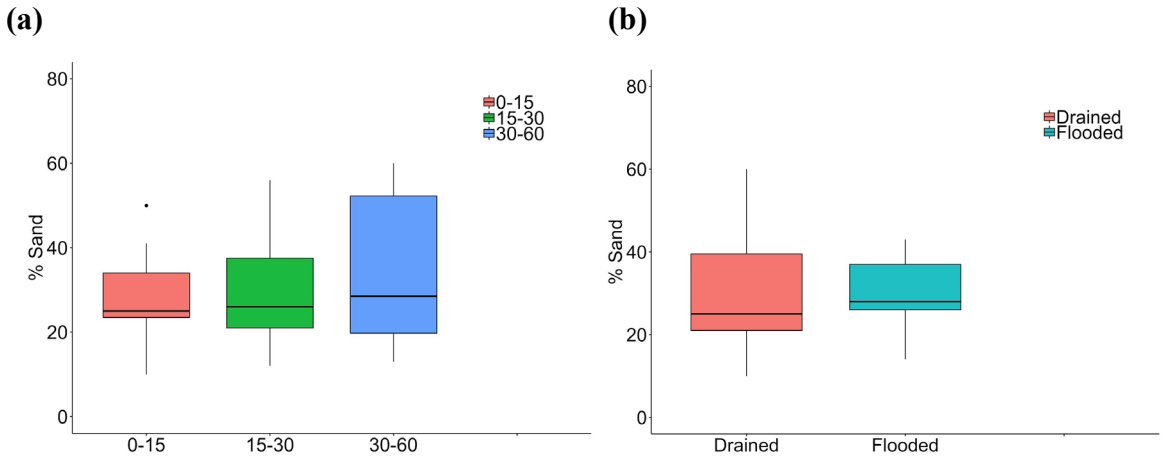

Figure 3. Difference in silt content across soil depth and flooding status. Box-and-whisker plot comparisons of percent sand content values across: (a) depth categories of 0-15, 15-30, and 30-60 cm and (b) drained and flooded soils. The box indicates the middle 50% (between 1st and 3rd quartile) of data values, the top whisker indicates the upper 25% of data valued, and the bottom whisker indicates the lowest 25% of data values. Outliers (values great than 1.5 times the interquartile range above the median or less than 1.5 times the interquartile range below the median) are included in the whiskers.

Soil Carbon Values

Soil C results had no significance across the various depths, with mean values of 9.1% +/- 0.8% at 0-15 cm, 9.7% +/- 0.8% at 15-30 cm, and 8.6% +/- 1.95% at 30-60 cm. At 30-60 cm, there was a larger range in values when compared to the 0-15 cm and 15-30 cm (Figure 4a). There were significant differences across drained (mean +/- SE: 8.5% +/- 0.7%) and flooded (mean +/- SE: 12.5% +/- 0.7%) soils. Flooded soils had more C and a lower range than drained soils (Figure 4b).

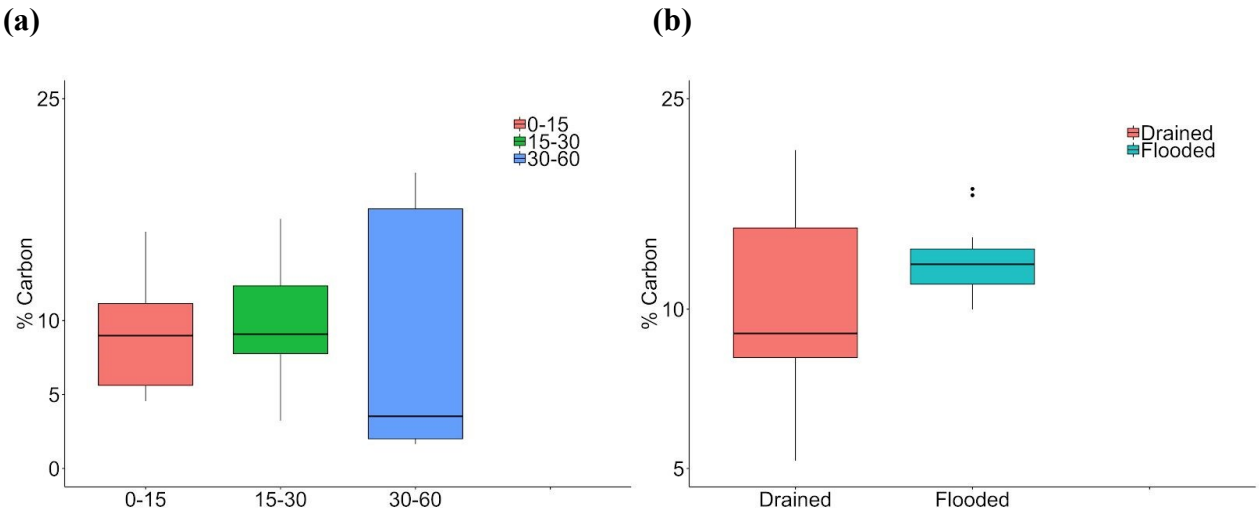

Figure 4. Difference in soil carbon values across soil depth and flooding status. Box-and-whisker plot comparisons of percent soil C values across: (a) depth categories of 0-15, 15-30, and 30-60 cm and (b) drained and flooded soils. The box indicates the middle 50% (between 1st and 3rd quartile) of data values, the top whisker indicates the upper 25% of data valued, and the bottom whisker indicates the lowest 25% of data values. Outliers (values great than 1.5 times the interquartile range above the median or less than 1.5 times the interquartile range below the median) are included in the whiskers.

Relationships Between Soil Texture and Soil Carbon

Clay

Clay is not a good predictor of soil C values across depths in all samples (Figure 5a). The R^2 value for the 0-15 cm depth was 0.009. The R^2 value for 15-30cm depth was 0.00.The R^2 value for 30-60cm depth was 0.01. When analyzed as drained or flooded soils, there was negative correlation in flooded soils between percent C content and percent clay content across the various depths (Figure 5b). There was no clear correlation for drained soils.

(a) **(b)**

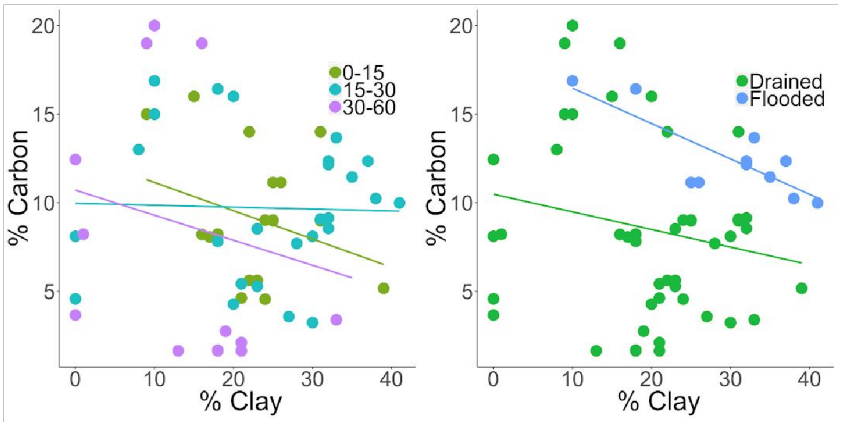

Figure 5. Correlation between clay content and carbon content across soil depth and flooding status. Scatter plot correlations between percent clay content and percent C content across: (a) depth categories of 0-15 (green), 15-30 (blue), and 30-60 cm (purple) and (b) drained (green) and flooded (blue) soils. Percent (%) clay content is on the x-axis and percent (%) carbon content is on the y-axis. Colored dots represent individual data points in the different depth or flooding status categories. Solid lines represent correlation trends between data points of each category.

Silt

Silt is not a good predictor of soil C values across depths in all samples (Figure 6a). The R^2 value for the 0-15 cm depth was 0.44. The R^2 value for 15-30cm depth was 0.27. The R^2 value for 30-60cm depth was 0.85. Negative trends were seen across all three depths, with the strongest negative trend in 30-60cm and the weakest negative trend at 0-15cm. When analyzed as drained or flooded soils, there was negative correlation in drained soils between percent C content and percent clay content across the various depths (Figure 6b). There was no clear correlation for flooded soils.

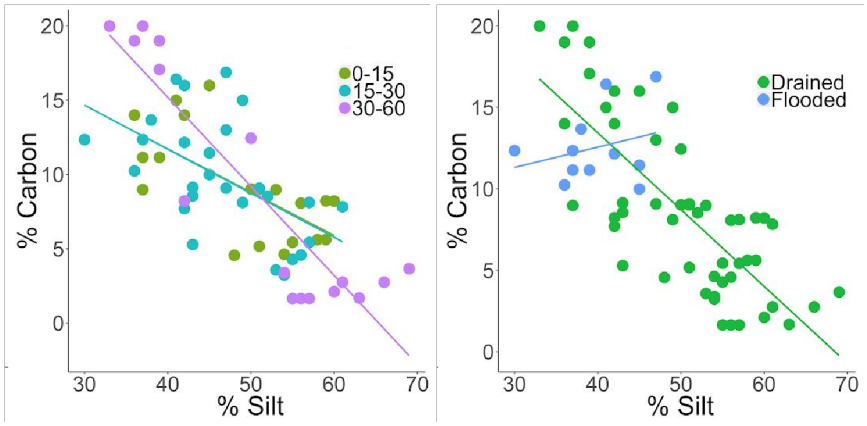

Figure 6. Correlation between silt content and carbon content across soil depth and flooding status. Scatter plot correlations between percent silt content and percent C content across: (a) depth categories of 0-15 (green), 15-30 (blue), and 30-60 cm (purple) and (b) drained (green) and flooded (blue) soils. Percent (%) clay content is on the x-axis and percent (%) carbon content is on the y-axis. Colored dots represent individual data points in the different depth or flooding status categories. Solid lines represent correlation trends between data points of each category.

Sand

Sand is a good predictor of soil C values across depths in all samples. The R^2 value for the 0-15 cm depth was 0.66. The R^2 value for 15-30cm depth was 0.13.The R^2 value for 30-60cm depth was 0.53. Positive trends in soil C values were seen across all three depths (Figure 7a). When analyzed as drained or flooded soils, there was positive correlation in flooded soils between percent C content and percent sand content across the various depths. There was a slight positive correlation for drained soils (Figure 7b).

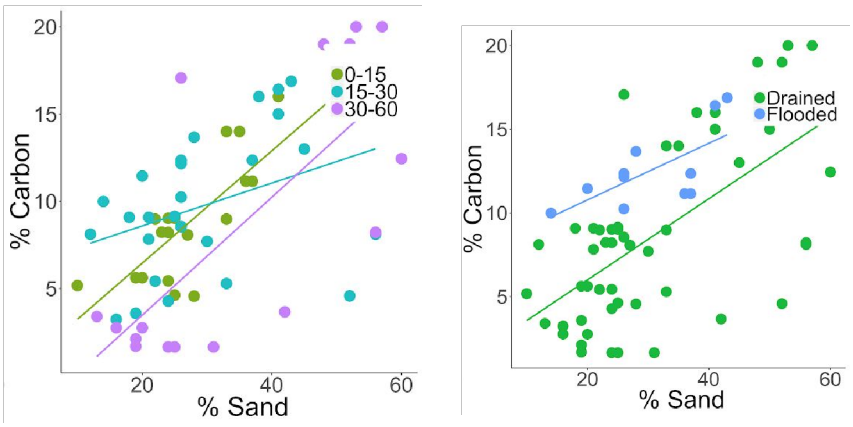

Figure 7. Correlation between sand content and carbon content across soil depth and flooding status. Scatter plot correlations between percent sand content and percent C content across: (a) depth categories of 0-15 (green), 15-30 (blue), and 30-60 cm (purple) and (b) drained (green) and flooded (blue) soils. Percent (%) clay content is on the x-axis and percent (%) carbon content is on the y-axis. Colored dots represent individual data points in the different depth or flooding status categories. Solid lines represent correlation trends between data points of each category.

DISCUSSION

Although the negative correlation between clay content and soil C rejects the hypothesis, positive sand and negative silt trends with soil C illustrate the importance of minerals and management practices in soil C trends. Additionally, flooded soils will exhibit higher rates of C sequestration when compared to trends among drained soils. Soil texture analysis results highlight different trends in clay, sand and silt content and broaden the understanding of the potential for C sequestration in Delta peatland soils.

Clay

Negative trends were surprising as they rejected the hypothesis that predicted increasing soil C with increasing clay content: clay soils typically hold more soil C**.** Intense industrial agriculture practices in the Delta may partly account for lower overall soil C levels. Soil C reduction may have also occurred in clay, thus reducing the amount of soil C detected. This trend contradicts other findings that suggest increased clay content correlates with increased soil C content, and illustrates how agricultural abuse can reduce soil C levels (Schimel et al. 1994). The

direct protection of soil C via flooding, rather than mineral protection from clay, reverses Delta peatland subsidence due to decreased soil C oxidation (Deverel 2016, Syvitski et al. 2009). Additionally, recently drained soils have less time for soil C to be oxidized when compared to earlier drained sites (Deverel and Leighton 2010).

Silt

Negative silt content and soil C correlations were also surprising because silt and clay coupled together may be better predictors of soil C content rather than silt alone. Predominantly comprised of iron, aluminum and silica minerals, weathered silt may also be a source of redox active minerals (Brady and Weil 2009). These redox active minerals are utilized by microbes to perform anaerobic respiration with soil C as a substrate that would otherwise be protected by flooding (Hall and Silver 2013). Additionally**,** soils with a higher silt content are less able to protect soil C compared to soils with a higher percentage of clay minerals.

Sand

Soils with high sand content also had higher soil C values even though the low surface area of sand particles typically does not protect residual soil C. Sand is usually comprised of unreactive minerals such as quartz. Thus, sand is not a source of redox active minerals that fuel microbial activity and limit soil C sequestration. Thus, flooded sandy soils have higher potential rates of soil C storage, which explain the observed trends between sand and soil C values. However, when these soils are drained the soil C is unprotected leading to higher rates of soil C loss from oxidation. Sand is positively correlated with soil C, but sand is not an important protector of residual soil C in the Delta system.

Limitations

Limitations of this analysis include a smaller sample size of flooded soils than desired, inability to collect flooded soils at lower depths and not enough sample material to conduct soil

texture analysis. We were unable to properly elaborate on the impacts of flooding on soil C sequestration because our sample size of flooded soils was significantly smaller (n=11) than the sample size of drained soils (n=51). This made it difficult to remove the effects of site mineralogy when comparing drained and flooded soils. For flooded soil collection, our sampling tools limited sample collection at deeper depths. Of the soil samples collected, we only ran soil texture analyses on 65 samples with masses greater than 50g.

Future Directions

A future study with a larger sample set, and more flooded soils samples, may provide a more comprehensive picture of the impacts of Delta flood regimes on soil C sequestration. Future research can also identify the pathways of other greenhouse emissions such as nitrous oxide and methane. Lastly, we can couple the impacts of redox reactions and soil texture on the production of greenhouse gas emissions.

CONCLUSION

Soils with more minerals, either clay or silt, have lower levels of soil C. Clay and silt of both drained and flooded soils may also further fuel soil C loss via anaerobic microbial activity. Soils with high soil C content have limited mineral-associated protections, with flooding being the most important protector of soil C. Soils with lower amounts of minerals are the best options for soil C sequestration via flooding because these soils have reduced residual soil C loss and the highest capacity to accumulate future soil C. In this dynamic and redox active Delta environment, clay is not a good predictor of soil C. Other variables controlling soil or redox state, including management, may play a bigger role in determining soil C sequestration rates. Management practices, including reflooding organic rich soils, are the best options for maximum soil C sequestration.

ACKNOWLEDGEMENTS

Thank you to my mentor Tyler Anthony who gave me the opportunity to do this project and provided me with months of support through the experimentation, data analysis, and writing processes of this project. The Silver Lab provided immense support, encouragement and guidance throughout this project. Vanessa Suarez kept me motivated and kept me company during long days in the lab and into the night at Moffitt Library, and she is one of my inspirations. Kurt Spreyer and Tina Mendez helped me complete this project by providing me guidance and mentorship. Tina especially took the time to structure my thesis and give me feedback that greatly improved my thesis. My communities in the SCECon 2019 planning team and Our Monologues showed me immense love and never failed to support me whenever I doubted myself along the process. Thank you to my friends who took the time to edit, Saba and Alicia, for helping transform my writing and communicate my research effectively. Thank you to my friends who have all supported me during this process: Dante, Jed, Jessie, Rizza, Amayrani, Alicia, Neena, Vanessa, Verity and many others. Lastly, thank you to my family for always supporting me and believing I could succeed at UC Berkeley and in my life. Special thanks to my dad, who never failed to motivate me after frantic phone calls and has always showed me love.

REFERENCES

Baldocchi, Dennis. Trials and Tribulations of Measuring Greenhouse Gas (CO 2, CH 4, H 2 O) Fluxes over a Drained Peatland. USGS, 2011, Trials and Tribulations of Measuring Greenhouse Gas (CO 2, CH 4, H 2 O) Fluxes over a Drained Peatland.

Brady, N. C., and R. R. Weil. 2009. Elements of the nature and properties of soils. Third edition. Pearson Educational International. Boston, MA.

Chamberlain, S. D., T. L. Anthony, W. L. Silver, E. Eichelmann, K. S. Hemes, P. Y. Oikawa, C. Sturtevant, D. J. Szutu, J. G. Verfaillie, and D. D. Baldocchi. 2018. Soil properties and sediment accretion modulate methane fluxes from restored wetlands. Global Change Biology 24:4107–4121.

Deverel, S. J., and D. A. Leighton. 2010. Historic, Recent, and Future Subsidence, Sacramento-San Joaquin Delta, California, USA. San Francisco Estuary and Watershed Science 8.

Deverel, S. J., C. E. Lucero, and S. Bachand. 2015. Evolution of Arability of Land Use, Sacramento-San Joaquin Delta, California. San Francisco Estuary and Watershed Science 13.

Deverel, S. J., T. Ingrum, and D. Leighton. 2016. Present-day oxidative subsidence of organic soils and mitigation in the Sacramento-San Joaquin Delta, California, USA. Hydrogeology Journal 24:569–586.

Deverel, S., T. Ingrum, C. Lucero, and J. Drexler. 2014. Impounded Marshes on Subsided Islands: Simulated Vertical Accretion, Processes, and Effects, Sacramento-San Joaquin Delta, CA USA. San Francisco Estuary and Watershed Science 12.

Delta Protection Commission (2012) Economic Sustainability Plan for the Sacramento-San Joaquin Delta.

Drexler, J. Z., C. S. Fontaine, and S. J. Deverel. 2009. The legacy of wetland drainage on the remaining peat in the Sacramento — San Joaquin Delta, California, USA. Wetlands 29:372–386.

Eichelmann, E., K. S. Hemes, S. H. Knox, P. Y. Oikawa, S. D. Chamberlain, C. Sturtevant, J. Verfaillie, and D. D. Baldocchi. 2018. The effect of land cover type and structure on evapotranspiration from agricultural and wetland sites in the Sacramento–San Joaquin River Delta, California. Agricultural and Forest Meteorology 256-257:179–195.

Fleck, J. A., D. A. Bossio, and R. Fujii. 2004. Dissolved Organic Carbon and Disinfection By-Product Precursor Release from Managed Peat Soils. Journal of Environment Quality 33:465.

Hall, S. J., and W. L. Silver. 2013. Iron oxidation stimulates organic matter decomposition in humid tropical forest soils. Global Change Biology 19:2804–2813.

Hemes, K. S., S. D. Chamberlain, E. Eichelmann, T. Anthony, A. Valach, K. Kasak, D. Szutu, J. Verfaillie, W. L. Silver, and D. D. Baldocchi. 2019. Assessing the carbon and climate benefit of restoring degraded agricultural peat soils to managed wetlands. Agricultural and Forest Meteorology 268:202–214.

JMP® Pro, Version 13. SAS Institute Inc., Cary, NC, 1989-2019.

Knox, S. H., C. Sturtevant, J. H. Matthes, L. Koteen, J. Verfaillie, and D. Baldocchi. 2014. Agricultural peatland restoration: effects of land-use change on greenhouse gas (CO2 and CH4) fluxes in the Sacramento-San Joaquin Delta. Global Change Biology 21:750–765.

Landry, J., and L. Rochefort. 2012. The Drainage of Peatlands: impacts and rewetting techniques. Peatland Ecology Research Group. Québec.

Leifeld, J., and L. Menichetti. 2018. The underappreciated potential of peatlands in global climate change mitigation strategies. Nature Communications 9.

Miller, R., M. S. Fram, R. Fujii, and G. Wheeler. 2008. Subsidence Reversal in a Re-Established Wetland in the Sacramento-San Joaquin Delta, California, USA. San Francisco Estuary and Watershed Science 6.

Moore, T. R., and M. Dalva. 1993. The influence of temperature and water table position on carbon dioxide and methane emissions from laboratory columns of peatland soils. Journal of Soil Science 44:651–664.

Pronger, J., L. A. Schipper, R. B. Hill, D. I. Campbell, and M. Mcleod. 2014. Subsidence Rates of Drained Agricultural Peatlands in New Zealand and the Relationship with Time since Drainage. Journal of Environment Quality 43:1442.

Ramchunder, S., L. Brown, and J. Holden. 2009. Environmental effects of drainage, drain-blocking and prescribed vegetation burning in UK upland peatlands. Progress in Physical Geography: Earth and Environment 33:49–79.

Schimel, D. S., B. H. Braswell, E. A. Holland, R. Mckeown, D. S. Ojima, T. H. Painter, W. J. Parton, and A. R. Townsend. 1994. Climatic, edaphic, and biotic controls over storage and turnover of carbon in soils. Global Biogeochemical Cycles 8:279–293.

Silvola, J., J. Alm, U. Ahlholm, H. Nykänen, and P. J. Martikainen. 1996. The contribution of plant roots to CO2 fluxes from organic soils. Biology and Fertility of Soils 23:126–131.

Smith, P. 2004. Carbon sequestration in croplands: the potential in Europe and the global context. European Journal of Agronomy 20:229–236.

Syvitski, J. P. M., A. J. Kettner, I. Overeem, E. W. H. Hutton, M. T. Hannon, G. R. Brakenridge, J. Day, C. Vörösmarty, Y. Saito, L. Giosan, and R. J. Nicholls. 2009. Sinking deltas due to human activities. Nature Geoscience 2:681–686.

APPENDIX A: Site Map

Figure A1. Map of the central Sacramento-San Joaquin Delta, California outlining the nine sampling locations. Each numbered blue label represents a different sampling site, with label #8 representing both Sherman and Sherman Pasture sampling sites. Generated by T. Anthony using Google Maps.

APPENDIX B: Hydrometer Protocol

Protocol to determine soil texture via. hydrometer method. Purpose is to measure soil texture by the hydrometer method.

Materials

1. Sieved soil (50 g dry wt equivalent if fine-textured, 100 g if sandy).
2. Electric mixer and cup.
3. Sedimentation cylinder (1000 mL).
4. Bouyoucos hydrometer.
5. Thermometer (-20° - 110°C).

Reagents

1. Sodium hexametaphosphate, 1*N*.

Procedure

NOTE: If soil is not oven dried, take a subsample for water content determination.

1. Place 50 - 100 g of soil (dry weight equivalent) into a soil dispersing cup. Record the weight to at least 0.1g.
2. Fill cup to within two inches of the top with tap water. If local tap water is hard, use distilled water. Water should be at room temperature, not directly out of tap.
3. Add 5 ml of 1*N* sodium hexametaphosphate.
4. Allow to slake (soak) for 15 minutes (high-clay soils only).
5. Attach cup to mixer; mix 5 minutes for sandy soils, 15 minutes for fine-textured soils.
6. Transfer suspension to sedimentation cylinder; use tap water from squirt bottle to get all of sample from mixing cup.
7. Fill cylinder to 1000-mL mark with tap water.
8. CAREFULLY mix suspension with plunger. After removing plunger, begin timing. Carefully place hydrometer into suspension; note reading at 40 seconds. This 40-second

reading should be repeated several times to improve accuracy. Because the suspension is opaque, read the hydrometer at the top of the meniscus rather than at the bottom.

9. After final 40-second reading, remove hydrometer, carefully lower a thermometer into the suspension and record the temperature (°C). Mixing raises temperature by 3-5°C, so it is important to record the temperature for both hydrometer readings (40 sec and 2 hr).
10. Mix suspension again and begin timing for the two-hour reading. Be sure that the cylinder is back from the edge of the counter and in a location where it won't be disturbed.
11. Make up a blank cylinder with water and sodium hexametaphosphate. Record the blank hydrometer reading. If the reading is above 0 (zero) on the hydrometer scale (in other words, if the zero mark is below the surface), record the blank correction as a negative number. Read at the top of the meniscus as before.
12. Take a hydrometer reading at 2 hours, followed by a temperature reading.